

# Three-dimensional chiral skyrmions with attractive interparticle interactions

A O Leonov,<sup>1,2,3,\*</sup> T L Monchesky,<sup>1,4</sup> J C Loudon,<sup>5</sup> and A N Bogdanov<sup>1,2</sup>

<sup>1</sup>Center for Chiral Science, Hiroshima University, Higashi-Hiroshima, Hiroshima 739-8526, Japan

<sup>2</sup>IFW Dresden, Postfach 270016, D-01171 Dresden, Germany

<sup>3</sup>Zernike Institute for Advanced Materials, University of Groningen, Groningen, 9700AB, The Netherlands

<sup>4</sup>Department of Physics and Atmospheric Science,  
Dalhousie University, Halifax, Nova Scotia, Canada B3H 3J5

<sup>5</sup>Department of Materials Science and Metallurgy,  
27 Charles Babbage Road, Cambridge, CB3 0FS, United Kingdom

(Dated: February 9, 2016)

We introduce a new class of isolated three-dimensional skyrmion that can occur within the cone phase of chiral magnetic materials. These novel solitonic states consist of an axisymmetric core separated from the host phase by an asymmetric shell. These skyrmions attract one another. We derive regular solutions for isolated skyrmions arising in the cone phase of cubic helimagnets and investigate their bound states.

PACS numbers: 75.30.Kz, 12.39.Dc, 75.70.-i.

The *Dzyaloshinskii-Moriya* (DM) interaction in non-centrosymmetric magnets is a result of their crystallographic handedness<sup>1</sup> and is responsible for the formation of long-range modulations with a fixed sense of the magnetization rotation<sup>1,2</sup> and the stabilization of two-dimensional axisymmetric localized structures called *skyrmions*<sup>3,4</sup>. Long-range homochiral modulations (*helices*) were found in the noncentrosymmetric cubic ferromagnet MnSi several decades ago and since then, other cubic ferromagnets with B20 structures have been investigated intensively<sup>5-7</sup> as have other chiral magnetic materials<sup>8,9</sup>. Isolated chiral skyrmions have been discovered recently in PdFe/Ir(111) nanolayers with induced DM interactions and strong easy-axis anisotropy<sup>10-12</sup>.

Chiral skyrmions are two-dimensional topological solitons with an axisymmetric structure localized in nanoscale cylindrical regions. They exist as ensembles of weakly repulsive particles in the *saturated* phase of non-centrosymmetric magnets<sup>4,13,14</sup> in which all the atomic spins are parallel to an applied magnetic field. In cubic helimagnets, below a certain critical field,  $H_D$ , the saturated phase transforms into the chiral helical state with the propagation direction along the applied field called the *cone* phase<sup>2</sup>. Unlike the saturated phase, the boundary values imposed by the longitudinal modulations of the cone phase violate a rotational symmetry of the system, and are thus incompatible with the axisymmetric arrangement of skyrmions investigated in Refs. 4, 10, 11, and 13. Then, the question arises: “are there any localized states compatible with the encompassing cone phase?”

In our report we address this compatibility problem and derive regular solutions for asymmetric skyrmions embedded into the cone phase. We demonstrate that unlike the repulsive axisymmetric skyrmions existing in the saturated states, chiral solitons in the cone phase have an attractive interskyrmion potential and form biskyrmion and multiskyrmion states.

We consider the standard model for magnetic states in

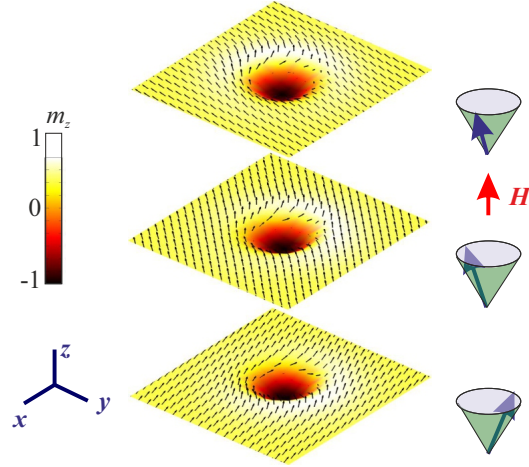


FIG. 1. (color online). Magnetic structure of an isolated skyrmion in the cone phase: calculated contour plots of  $m_z(x, y)$  in three layers with  $\Delta\psi_c = 2\pi/3$ . Details of the magnetization distribution are given in Fig. 2.

cubic non-centrosymmetric ferromagnets<sup>1,2</sup>,

$$w = A(\mathbf{grad} \mathbf{m})^2 + D \mathbf{m} \cdot \mathbf{rot} \mathbf{m} - \mu_0 M \mathbf{m} \cdot \mathbf{H}, \quad (1)$$

where  $\mathbf{m} = (\sin \theta \cos \psi; \sin \theta \sin \psi; \cos \theta)$  is the unity vector along the magnetization  $\mathbf{M}$ ,  $A$  is the exchange stiffness constant,  $D$  is the Dzyaloshinskii-Moriya (DM) coupling energy, and  $\mathbf{H}$  is the applied magnetic field.

Chiral modulations along the applied field with the period  $L_D = 4\pi A/|D|$  correspond to the global minimum of the functional (1) below the critical field  $\mu_0 H_D = D^2/(2AM)$ . The equilibrium parameters for the cone phase are expressed in analytical form<sup>2</sup> as:

$$\theta_c = \arccos(H/H_D), \quad \psi_c = 2\pi z/L_D, \quad (2)$$

where  $z$  is the spatial variable along the applied field.

At  $H = H_D$ , the cone phase transforms into the saturated state with  $\theta = 0$ . Within the saturated phase

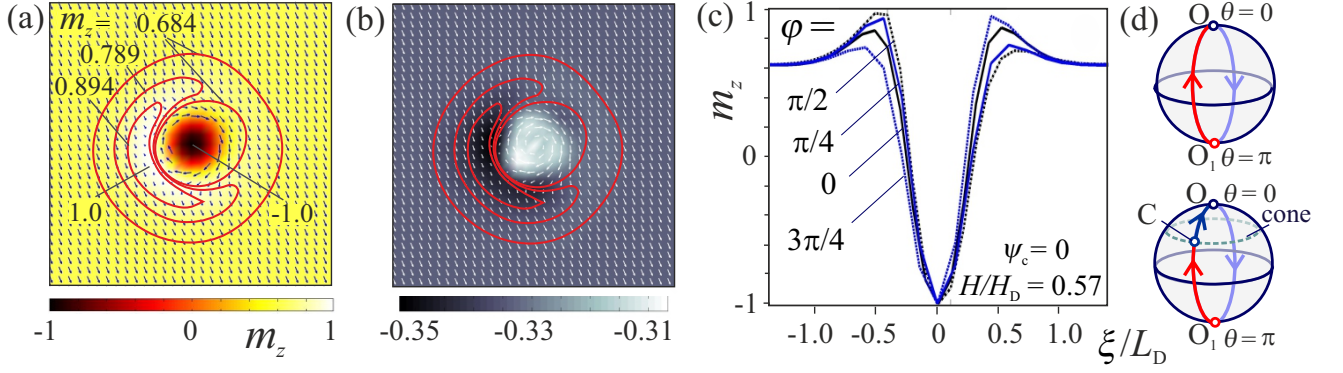


FIG. 2. (color online) Numerical solutions for asymmetric skyrmions (5) for  $H = 0.57H_D$ : contour plots of  $m_z(x, y)$  (a) and energy density  $e(x, y)$  (b) in a  $xy$  plane with a fixed value of  $\psi_c$  (2); (c) magnetization profiles  $\theta(r)$  for different values of  $\varphi$  in the  $xy$  layer with  $\psi_c = 0$  ( $\xi$  is the spatial variable along lines with fixed values of  $\varphi$ ); (d) trajectories of the magnetization vector  $\mathbf{m}$  for axisymmetric skyrmions (4) (top) and for asymmetric localized solitons (5) along the line  $\varphi = \psi_c + \pi/2$  (bottom).

( $H > H_D$ ), isolated chiral skyrmions are described by axisymmetric solutions of type

$$\theta = \theta(\rho), \quad \psi = \varphi + \pi/2, \quad (3)$$

that are homogeneous along the skyrmion axis  $z$  where  $\mathbf{r} = (\rho \cos \varphi, \rho \sin \varphi, z)$  are cylindrical coordinates for the spatial variable<sup>4</sup>. The equilibrium solutions for  $\theta(\rho)$  are derived from the Euler equation for the energy functional<sup>4</sup>

$$w_s(\theta) = A\mathcal{J}_0(\theta) + D\mathcal{I}_0(\theta) - \mu_0 MH \cos \theta, \\ \mathcal{J}_0(\theta) = \theta_\rho^2 + \frac{1}{\rho^2} \sin^2 \theta, \quad \mathcal{I}_0(\theta) = \theta_\rho + \frac{1}{\rho} \sin \theta \cos \theta, \quad (4)$$

with the boundary conditions  $\theta(0) = \pi$ ,  $\theta(\infty) = 0$  (see Fig. 3 (i)-(l) for the distribution of the  $m_z$ -component of the magnetization and energy density distributions in a  $xy$  plane with a fixed value of  $z$ ).

Below the saturation field ( $H < H_D$ ), the structure of two-dimensional skyrmions is imposed by the arrangement of the cone phase (2). These solutions should be periodic with period  $L_D$  along the  $z$ -axis and are confined by the following in-plane boundary conditions:

$$\theta_{\rho=0} = \pi, \quad \theta_{\rho=\infty} = \theta_c, \quad \psi_{\rho=\infty}(z) = \psi_c(z). \quad (5)$$

The solutions for  $\theta(\rho, \varphi, z)$ ,  $\psi(\rho, \varphi, z)$  are derived by minimization of the energy functional (1):

$$w = A\mathcal{J}(\theta, \psi) + D\mathcal{I}(\theta, \psi) - \mu_0 MH \cos \theta, \quad (6)$$

with the boundary conditions (5), where the exchange ( $\mathcal{J}$ ) and Dzyaloshinskii-Moriya ( $\mathcal{I}$ ) energy functionals are

$$\mathcal{J}(\theta, \psi) = \theta_\rho^2 + \theta_z^2 + \frac{1}{\rho^2} \theta_\varphi^2 + \sin^2 \theta \left( \psi_\rho^2 + \psi_z^2 + \frac{1}{\rho^2} \psi_\varphi^2 \right), \\ \mathcal{I}(\theta, \psi) = \sin(\psi - \varphi) \left( \theta_\rho + \frac{1}{\rho} \sin \theta \cos \theta \psi_\varphi \right) + \sin^2 \theta \psi_z \\ + \cos(\psi - \varphi) \left( \frac{1}{\rho} \theta_\varphi + \sin \theta \cos \theta \psi_\rho \right).$$

To investigate the solutions for asymmetric skyrmions, we use both the continuous and the discretized versions

of Eq. (1). In the continuous version, we use finite-difference approximation of derivatives in Eq. (1) with different precision up to eight points as neighbors on rectangular grids with adjustable grid spacings. The size of the grid is up to  $150 \times 150 \times 100$ . In the discretized version, we consider classical spins of unit length on a three-dimensional cubic lattice with the following energy functional:

$$w = - \sum_{\langle i, j \rangle} (\mathbf{S}_i \cdot \mathbf{S}_j) - \sum_i \mathbf{h} \cdot \mathbf{S}_i \\ - d \sum_i (\mathbf{S}_i \times \mathbf{S}_{i+\hat{x}} \cdot \hat{y} - \mathbf{S}_i \times \mathbf{S}_{i+\hat{y}} \cdot \hat{x}) \quad (7)$$

where  $\mathbf{h} = \mathbf{H}J/D^2$  and  $d = J/D = 1/\tan(2/p)$ .  $\langle i, j \rangle$  denotes pairs of nearest-neighbor spins. The Dzyaloshinskii-Moriya constant  $d$  defines the period of modulated structures  $p$ . Or vice versa, one chooses the period of the modulations for the computing procedures and defines the corresponding value of  $d$ . In what follows, the Dzyaloshinskii-Moriya constant is set to 0.7265 which corresponds to one-dimensional modulations with a period of 10 lattice spacings in zero field. The discrete model (7) is particularly useful when the continuum model becomes invalid for localized solutions with sizes of few lattice constants<sup>12,15</sup>. The model also allows to operate with smaller arrays of spins as compared with the continuum model.

Numerical calculations for  $H = 0.57H_D$  (Figs. 1, 2) show the main features of asymmetric skyrmions. The entire structure of a skyrmion within the cone phase can be thought of as a stack of layers (Fig. 1) rotating around the  $z$  axis with period  $L_D$ . These specific solitonic states are characterized by three-dimensional chiral modulations: the cone modulations along their axis and a double-twist rotation in the perpendicular plane.

Figs. 2 (a-c) present the equilibrium structures of Eq. (7) within a layer with a fixed value of  $z$ . The function  $m_z(\rho, \varphi)$  consists of a strongly localized axisymmet-

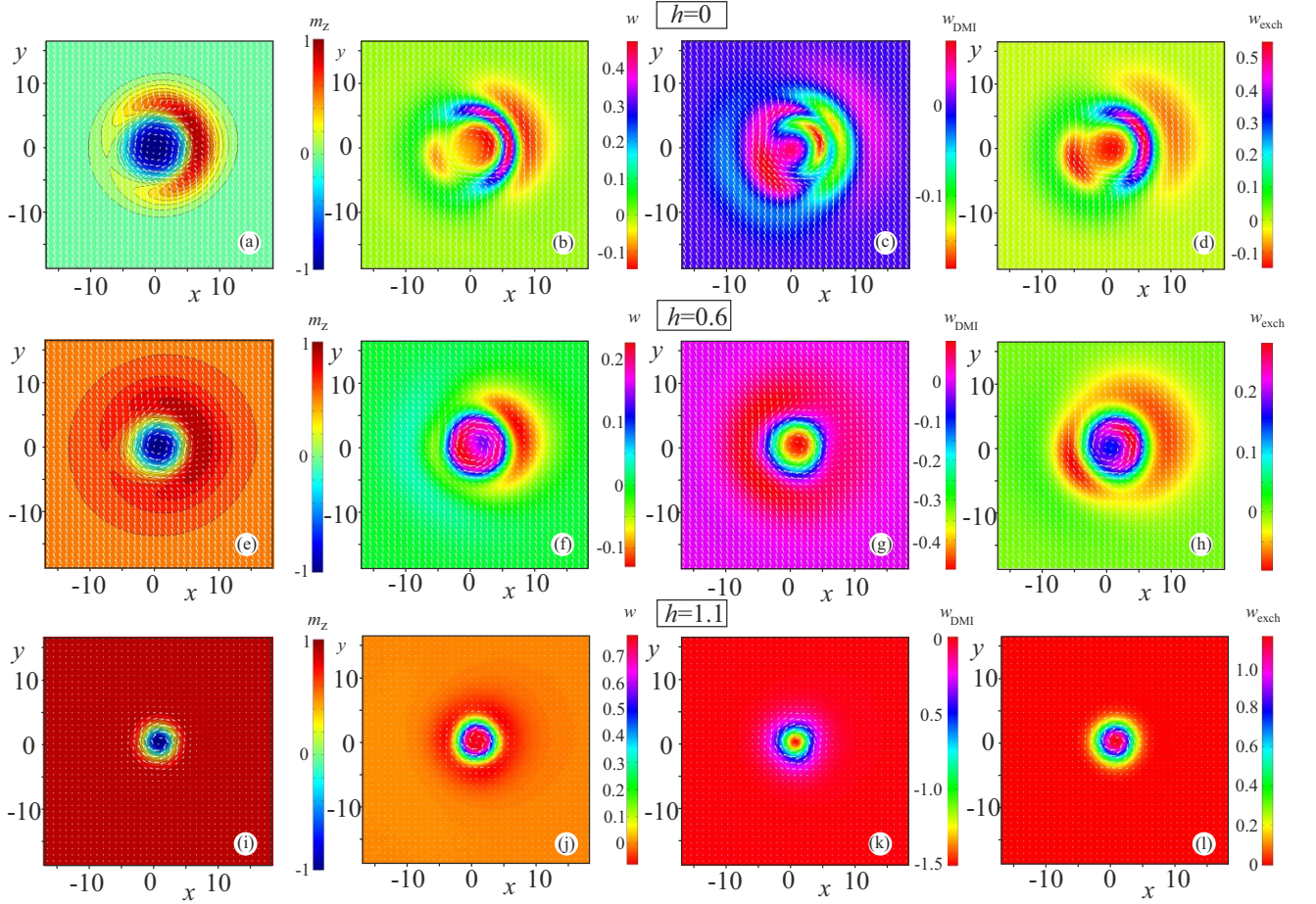


FIG. 3. (color online) Numerical solutions for asymmetric skyrmions (5) obtained within the continuum model (1) for different values of the applied magnetic field. Contour plots of  $m_z(x, y)$  (a), (e), (i), energy density  $w$  (b), (f), (j), energy density of DM (c), (g), (k), and exchange interaction (d), (h), (l) are plotted in a  $xy$  plane with a fixed value of  $\psi_c$  (2).

ric core separated from the outer region with a fixed value of the magnetization  $\mathbf{m}(\theta_c, \psi_c)$  (2) by a broad strongly asymmetric transitional region we call the *shell*.

The contour lines of equal  $m_z$  in Fig. 2 (a) and magnetization profiles along the skyrmion diameter,  $m_z(\xi)$  in Fig. 2 (c), display details of the shell. Note especially that the magnetization profile along  $\varphi = \psi_c + \pi/2$  reaches the value  $\theta = 0$ . In Fig. 2 (a), this point is enclosed by crescent-shaped contours. The unit spheres in Fig. 2 (d) demonstrate the difference between the solution for axisymmetric skyrmions in the saturated phase (3) and those within the cone phase (5). The former are described by  $OO_1$  lines connecting the skyrmion center with  $\theta = \pi$  ( $O_1$ ) and the point  $O$  corresponding to the system “vacuum”,  $\theta = 0$ . Solutions for skyrmions within the cone phase are described by the lines connecting the skyrmion center ( $O_1$ ) with the point  $C$  corresponding to the cone phase (2). In Fig. 2 (d) we indicate the magnetization trajectory along  $\varphi = \psi_c + \pi/2$  direction. Fig. 3 (the first column) shows the contour plots of  $m_z$  components refined within the continuous model (1) for different values of the applied magnetic field. The sec-

ond column shows the energy density  $w$  of Eq. (1) while the third and the fourth column show DM and exchange energy densities, correspondingly.

Fig. 4 shows the radial skyrmion energy density  $e(\rho) = (2\pi L_D)^{-1} \int_0^{L_D} dz \int_0^{2\pi} d\varphi w_s(\theta, \psi)$  for different values of the field as calculated with respect to the energy density of the conical phase. The positive exponentially decaying asymptotics of  $e(\rho)$  (Fig. 4 (a), (b)) imply the *attractive* interaction between the skyrmions in the cone phase, whereas the axisymmetric skyrmions in the saturated state of chiral magnets (Fig. 4 (c)) have a repulsive interskyrmion potential<sup>13,14,16</sup>.  $e(\rho)$  has three characteristic radii  $R_1$ ,  $R_2$ , and  $R_3$ , dependence of which on the field is plotted in Fig. 4 (d). The *shell* mentioned above is the part of the asymmetric skyrmion with  $\rho > R_3$ . Note, that the *shell* disappears in zero field as well as for  $h > 0.8$ . The characteristic radius  $R_2$  specifies the size of the skyrmionic *core* ( $0 < \rho < R_2$ ). We also call the part of the skyrmion with  $R_2 < \rho < R_3$  the *ring*. In Ref.<sup>14</sup> it was pointed out that this ring with the negative energy density due to the DM interaction guarantees the stability of the chiral skyrmion. Note that with decreasing



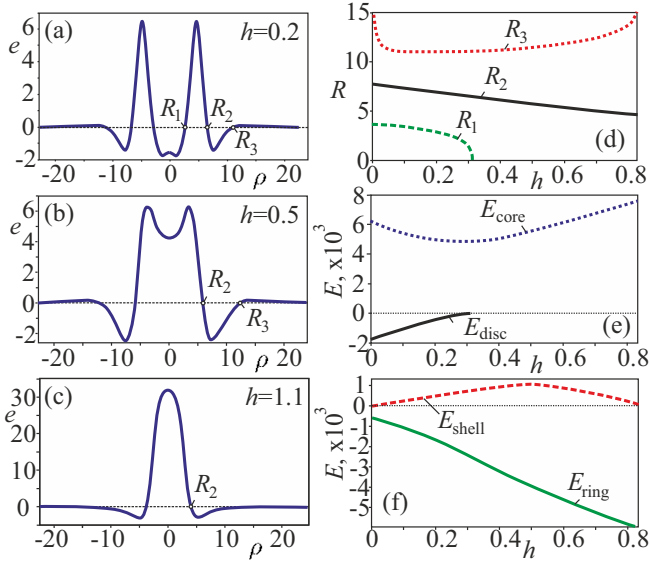


FIG. 4. (color online). Variation of the energy density  $e(\rho)$  along the skyrmion diameter, for different values of the applied magnetic field (a), (b), (c). (d) dependence of the characteristic radii  $R_1$ ,  $R_2$ ,  $R_3$  of the energy density  $e(\rho)$  from (a)-(c) on the field. The total energies  $E$  accumulated within the different parts of the asymmetric skyrmions in dependence on the field (e), (f). The Energy of the *disc*  $E_{disc}$  was integrated over the interval  $[0, R_1]$ , the energy of the *core*  $E_{core}$  - over  $[0, R_2]$ , the energy of the *ring*  $E_{ring}$  - in the interval  $[R_2, R_3]$ , and the energy of the *shell*  $E_{shell}$  - for  $\rho > R_3$ .

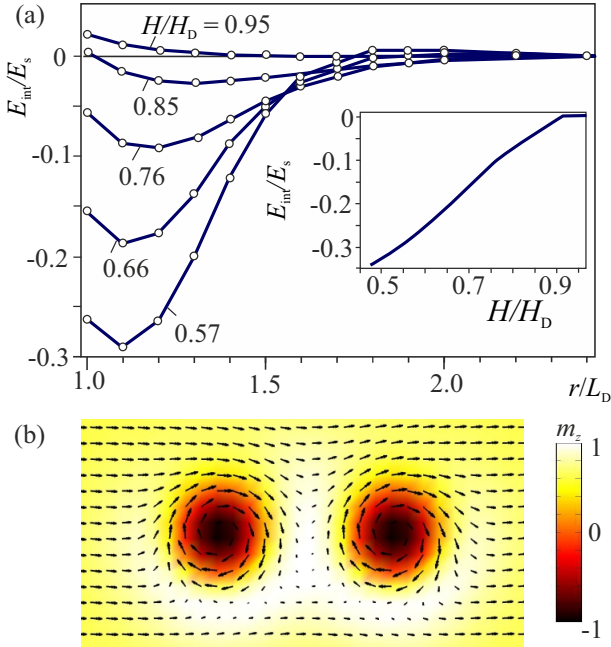


FIG. 5. (color online). Reduced energy for the interaction between two asymmetric skyrmions,  $E_{int}/E_s$ , as a function of the distance between the skyrmion centers  $r$  calculated for different values of the applied field (a). Inset shows minimal values of  $E_{int}$  as a function of the applied field. Contour plot of  $m_z(x, y)$  for bound asymmetric skyrmions at  $H/H_D = 0.57$  (b).

magnetic field a *disc* ( $\rho < R_1$ ) with the negative energy density develops. The total energies  $E$  accumulated within the different parts of the asymmetric skyrmions are shown in dependence on the field in Fig. 4 (e), (f).

In Fig. 5 (a) the reduced interaction energy between two asymmetric skyrmions,  $E_{int}/E_s$  is plotted as a function of their separation distance for different values of the applied magnetic field ( $E_s = \int_0^\infty e(\rho)\rho d\rho$  is the total equilibrium energy of an isolated asymmetric skyrmion). The Lennard-Jones type potential profiles  $E_{int}/E_s(r/L_D)$  show that the attractive interskyrmion coupling is characterized by a low potential barrier and a rather deep potential well establishing the equilibrium separation of skyrmions in the bound biskyrmion state (Fig. 5 (b)).

In conclusion, regular solutions for isolated chiral skyrmions in the cone phase of cubic helimagnets have been derived by numerically solving the corresponding micromagnetic equations (5) and (6). These novel solitonic states are characterized by three-dimensional chiral modulations and an attractive interskyrmion potential. Similar skyrmionic states can arise in the cone phases admissible in uniaxial chiral ferromagnets with  $C_n$  and  $D_n$  symmetry<sup>1,3</sup>. Axisymmetric skyrmions exist in the saturated phase of chiral ferromagnets as ensembles of repulsive isolated particles<sup>4,10,14</sup>. Our findings show that below the transition field into the cone phase, the axisymmetric skyrmions transform into asymmetric attractive solitons and may form biskyrmion and multiskyrmion states (clusters).

To date, no direct observations of isolated skyrmions or skyrmion clusters have been reported in the cone phases of chiral helimagnets. However, a few isolated observations such as a decomposition of a skyrmion lattice into cluster-like patterns<sup>17</sup> and the formation of skyrmionic droplets in MnSi plates<sup>18</sup>, are in accord with our theoretical results and indicate possible directions for the investigation of this phenomenon.

The authors are grateful to K. Inoue, J. Kishine, and G. Tatara for useful discussions. A.O.L acknowledges financial support by the FOM grant 11PR2928. A.N.B acknowledges support by the Deutsche Forschungsgemeinschaft via Grant No. BO 4160/1-1.

- 
- \* A.Leonov@ifw-dresden.de
- <sup>1</sup> Dzyaloshinskii I E 1964 Sov. Phys. JETP **19** 960
  - <sup>2</sup> Bak P and Jensen M H 1980 J. Phys.C: Solid State Phys. **13** L881
  - <sup>3</sup> Bogdanov A N and Yablonsky A D 1989 Sov. Phys. JETP **68** 101
  - <sup>4</sup> Bogdanov A and Hubert A 1994 J. Magn. Magn. Mater. **138** 255
  - <sup>5</sup> Ishikawa Y, Tajima K, Bloch D and Roth M 1976 Solid State Commun. **19** 525
  - <sup>6</sup> Beille J, Voiron J, Roth M and Zhang Z Y 1981 J. Phys. F: Met. Phys. **11** 2153
  - <sup>7</sup> Lebech B, Bernhard J and Freltoft T 1989 J. Phys.: Condens. Matter **1** 6105
  - <sup>8</sup> Togawa Y, Koyama T, Takayanagi K, Mori S, Kousaka Y, Akimitsu J, Nishihara S, Inoue K, Ovchinnikov A S and Kishine J I, 2012 Phys. Rev. Lett. **108** 107202
  - <sup>9</sup> Porter N A *et al* 2015 Phys. Rev. B **92** 144402
  - <sup>10</sup> Romming N, Hanneken C, Menzel M, Bickel J E, Wolter B, von Bergmann K, Kubetzka A, and Wiesendanger R 2013 Science **341** 636
  - <sup>11</sup> Romming N, Kubetzka A, Hanneken C, von Bergmann K, Wiesendanger R 2015 Phys. Rev. Lett. **114** 177203 ; Marrows C H 2015 Physics **8** 40
  - <sup>12</sup> A. O. Leonov, T. L. Monchesky, N. Romming, A. Kubetzka, A. N. Bogdanov, R. Wiesendanger arXiv: 1508.02155.
  - <sup>13</sup> Bogdanov A 1995 JETP Lett. **62** 247
  - <sup>14</sup> Rößler U K, Leonov A A, Bogdanov A N 2011 J. Phys.: Conf. Ser. **303** 012105
  - <sup>15</sup> Leonov A O, Mostovoy M 2015 Nat. Commun. **6** 8275
  - <sup>16</sup> Komineas S and Papanicolaou N 2015 Phys. Rev. B **92** 064412
  - <sup>17</sup> Yu X Z, Onose Y, Kanazawa N, Park J H, Han J H, Matsui Y, Nagaosa N and Tokura Y 2010 Nature (London) **465** 901
  - <sup>18</sup> Grigoriev S V, Potapova N M, Moskvina E V, Dyadkin V A, Dewhurst Ch and Maleyev S V 2014 JETP Lett. **100** 216